Response of buried pipelines located through liquefied and non-liquefied ground

Masakatsu Miyajima[I] and Masaru Kitaura[II]

ABSTRACT

The earthquake damage data in the 1964 Niigata Earthquake and the 1983 Nihonkai-Chubu Earthquake show that the pipeline damage were found near the boundary between the liquefied and non-liquefied areas. In this paper, main factors affecting the pipe failure located through both liquefied and non-liquefied ground are considered in connection with subsidence, buoyancy and seismic motion which is different from the motion of neighboring sites. Formulae obtained by using beam theory are presented and the response characteristics of pipelines are discussed. The results suggest that serious attention should be paid to vibration-induced strains during liquefaction.

INTRODUCTION

The liquefaction of sandy soil caused much damage to buried pipeline systems during the 1989 Loma Prieta Earthquake in the U.S.A. Pipeline damage induced by liquefaction has repeatedly occurred in several earthquakes, for example, in the 1964 Niigata Earthquake, the 1983 Nihonkai-Chubu Earthquake and so on. Effects of liquefaction are classified into three types as follows: Loss of bearing capacity and generation of buoyancy, large ground displacement, and large dynamic response of ground. These effects seem to be great at the boundary between liquefied and non-liquefied sites because of sharp change of the ground characteristics. It was very interesting to note that all of the damage to cast iron pipe occurred at liquefied sites and most of those occurred near the boundary between the liquefied and non-liquefied sites during the 1983 Nihonkai-Chubu Earthquake (Kitaura and Miyajima 1986).

The purposes of the present paper are to clarify pipe behavior through a boundary between liquefied and non-liquefied sites and to discuss characteristics of the failures of the pipelines buried in such areas.

I Assistant Professor, Kanazawa University, 2-40-20 Kodatsuno Kanazawa 920 JAPAN.

II Professor, Kanazawa University, ditto.

MATHEMATICAL TREATMENT

Fig. 1 shows analytical models for pipelines buried through a boundary between liquefied and non-liquefied ground. In case 1, the pipeline is assumed to be subjected to subsidence of the liquefied ground. In case 2 buoyancy effect is a governing factor. In case 3, the pipeline is subjected to a seismic motion which is different from the motion of the liquefied ground, while in case 2 buoyancy effect in a layer of the ground above the neighboring zones. In this last case, the superficial vibrating elastic plate which is subjected to a periodical driving force at both ends. In these three analytical models, the liquefied layer can be regarded as a horizontally pipe material and the pipe motion is assumed for the Characteristics of the pipe strains are analyzed in the two-dimensional plane mathematical models. In this investigation, the perfectly elastic behavior is assumed for the estimated by solving the following differential equations with suitable boundary conditions.

(1) Case 1

According to the schematic representation of case 1, as shown in Fig. 1 and upon the above several assumptions, the differential equations for case 1 may be expressed as follows:

$$EI\frac{d^4v_1}{dx^4}+K_{v1}v_1=K_{v1}V_1 \qquad (0<x<l) \quad (1)$$

$$EI\frac{d^4v_2}{dx^4}+K_{v2}v_2=0 \qquad (x>l) \quad (2)$$

The boundary conditions are

$$\frac{dv_1}{dx}=0,\ \frac{d^3v_1}{dx^3}=0 \qquad (x=0) \quad (3)$$

$$v_1=v_2,\ \frac{dv_1}{dx}=\frac{dv_2}{dx},\ \frac{d^2v_1}{dx^2}=\frac{d^2v_2}{dx^2},\ \frac{d^3v_1}{dx^3}=\frac{d^3v_2}{dx^3} \qquad (x=l) \quad (4)$$

$$v_2=0,\ \frac{dv_2}{dx}=0 \qquad (x=\infty) \quad (5)$$

respectively.

(2) Case 2

Supposing that the transverse displacement in the pipeline depends on buoyancy effect, the governing differential equations for case 2 may be given by

$$EI\frac{d^4v_1}{dx^4}+K_{v1}v_1=F \qquad (0<x<l) \quad (6)$$

$$EI\frac{d^4v_2}{dx^4}+K_{v2}v_2=0 \qquad (x>l) \quad (7)$$

The boundary conditions Eqs. (3), (4) and (5) are also available for the problem of case 2.

(3) Case 3

Since the schematic model of case 3 is taking account of the liquefaction in the superficial layer of the ground, including the original model presented by Nishio et al. (1987), the differential equation can be written in a form of

$$EA\frac{d^2u_1}{dx^2} - K_{u1}\,u_1 = -K_{u1}\,U_1 \qquad (0<x<l) \qquad (8)$$

$$EA\frac{d^2u_2}{dx^2} - K_{u2}\,u_2 = -K_{u2}\,U_2 \qquad (x>l) \qquad (9)$$

The boundary conditions are

$$\frac{du_1}{dx}=0 \qquad (x=0) \qquad (10)$$

$$u_1 = u_2,\quad \frac{du_1}{dx}=\frac{du_2}{dx} \qquad (x=l) \qquad (11)$$

$$\frac{du_2}{dx}=0 \qquad (x=L) \qquad (12)$$

where U_1 in Eq. (8) and U_2 in Eq. (9) are expressed as follows;

$$U_1 = \frac{\cos\left(\frac{2\pi x}{cT}\right)}{\cos\left(\frac{2\pi l}{cT}\right)}U_{s0} \qquad (13)$$

$$U_2 = U_{s0} \qquad (14)$$

where u, v = longitudinal and transverse displacements in the ground, E = young's modulus of the pipe material, A = cross-displacements in the pipeline, U, V = sectional area of the pipe, I = area moment of inertia of the pipe, K_u, K_v = equivalent spring constants of the longitudinal and transverse motions, F = a force caused by the buoyancy effect, c = longitudinal wave velocity which is given as $c^2 = E_s/\rho$ in which E_s is Young's modulus of soil and ρ is soil density, U_{s0} = displacement amplitude in non-liquefied superficial layer, T = period of shaking, $2l$ = width of the liquefied zone and L = pipe length. Subscripts 1 and 2 respectively correspond to the two sections.

APPLICATION OF ANALYTICAL SOLUTIONS TO THE PRACTICAL CASES

Soil spring constant shows non-linear characteristics with increasing soil displacement. However, the soil spring constant is assumed to be unchangeable irrespective of the relative displacement for simplicity in this paper. This

unchangeable value is called as equivalent soil spring constant. The equivalent soil spring constant for liquefiable ground depends on the degree of liquefaction of the soil. Initially, the bending pipe stresses due to subsidence of the ground induced by liquefaction are investigated in relation to the ratio of the equivalent soil spring constant K_1/K_2 for case 1. Fig. 2 shows the relationship between the maximum bending pipe stresses due to subsidence of the liquefied ground, and the width of the liquefaction zone. The pipelines used in this analysis are steel pipelines whose physical properties are listed in Table 1. The magnitude of subsidence of the liquefied ground is assumed to be 20 cm, and it is equivalent to a 2% subsidence of 10m liquefied layer. Yoshimi et al. concluded that the average vertical strain as a result of consolidation under the weight of the soil was 1% to 3% when a horizontal layer of loose saturated sand was liquefied to a depth of approximately 5m to 20m (Yoshimi et al. 1975). The experimental results presented by Lee and Albaisa (1974) also agree with the results indicated by Yoshimi et al. (1975). It can be seen from Fig. 4 that the higher the ratio of the equivalent soil spring constant is, which means smaller degree of liquefaction, the greater the maximum bending pipe stresses are. It is interesting to note that the maximum bending pipe stress for each ratio of the equivalent soil spring constant does not increase in areas of liquefied ground where the width exceeds 10m. The maximum bending stress exceeds the allowable bending stress of steel pipe (4,200kgf/cm^2) when the ratio of the equivalent soil spring constant is greater than 0.1, particularly at a width of liquefied zone less than 5 m except for the region near 0m. Fig. 3 shows the relationship between the displacement of the pipe and the width of the liquefied zone. It can be seen from this figure that the relative displacement between the ground and pipe is observed for relatively narrow width of the liquefied ground or low ratio of the equivalent soil spring constant. In case 1, the location where the maximum bending stress occurs, is nearer the boundary between the liquefied and non-liquefied ground, for greater width of the liquefied ground or higher ratio of the equivalent soil spring constant.

In case 2, the buoyancy effects of the pipelines during liquefaction are estimated by using the method described by Kitaura and Miyajima (1985). Fig. 4 shows the relationship between the maximum bending pipe stress due to buoyancy effects induced by liquefaction and the excess pore water pressure. Fig. 5 illustrates the relationship between the displacement of the pipe and the width of the liquefied ground. In this study, the equivalent soil spring constant of the liquefied soil is estimated by the empirical equation proposed by Yoshida and Uematsu (1978). It was noted that the pipe reached the ground surface in the area where the width of liquefied ground exceeded 10 m as shown in Fig. 5. Therefore, the maximum bending pipe stresses disappear for great width and high excess pore water pressure in Fig. 4. It is evident from Fig. 4 that the greater the width of the liquefied ground is, the higher the maximum bending stress are, that is, the greater the probability of failure of the pipe due to buoyancy effects. It is also interesting to note that the maximum bending pipe stresses occurred in the non-liquefied ground in case of great width of the liquefied ground. In these analyses, it is assumed that the duration of the liquefaction process is lengthy enough to allow the occurrence of pipe deformation. However, since the duration of liquefaction induced by an actual earthquake depends on the local soil conditions, the above may actually not be the cases in reality. In order to evaluate the pipeline response due to buoyancy effects more precisely, the dynamic analysis indicated by Kitaura et al. (1987) is preferable.

In case 3, the distribution of the axial pipe strain is shown in Fig. 6, in relation to the ratio of the equivalent soil spring constant K_1/K_2. Fig. 7 illustrates the

relationship between the maximum axial pipe strain and the ratio of the equivalent soil spring constant. The conditions for the ground and the magnitude of an earthquake used in these analyses are summarized in Table 2. It is evident from these figures that the maximum axial strains decrease and the location where the maximum strains occurs approaches the boundary of the ground with a decrease in the ratio. During liquefaction processes, not only the equivalent soil spring constant varies but also longitudinal wave velocity c varies. Therefore, the longitudinal wave velocity is assumed to be proportional to the fourth root of (1 - r), where r is the excess pore water pressure ratio because the longitudinal wave velocity is proportional to the square root of Young's modulus of soil, and the shear modulus of the soil is proportional to the square root of (1 - r). Moreover, Young's modulus is proportional to the shear modulus of the soil. Fig. 8 shows the distribution of the axial pipe strain in relation to the excess pore water pressure ratio. Fig. 9 illustrates the relationship between the maximum axial pipe strain and the excess pore water pressure ratio. Excess pore water pressure higher than 0.9 is not included in this analysis because the longitudinal wave cannot be transmitted in such soft ground. It is evident from these figures that the maximum axial pipe strain occurs at the liquefied ground near the boundary between the liquefied and non-liquefied ground. The maximum axial pipe strain corresponding to the value of 0.2 of excess pore water pressure ratio is markedly great. This can be explained as follows: Fig 10 shows the magnification ratio of response displacement in a superficial layer. In this analysis, $1/(cT/2)$ is less than 1.0; therefore, the magnification ratio increases sharply with an increase in $1/(cT/2)$, i.e. with a decrease in c. However, in this case the magnification ratio decreases because $1/(cT/2)$ is greater than 1.0. Effects of the resonance of the liquefied ground are great when excess pore water pressure ratio is equal to 0.2. Furthermore, Fig. 10 suggests that care should also be taken in evaluating the resonance of the liquefied ground for greater width of liquefied ground than that in this analysis. The above results obtained by mathematical analyses suggest that the probability of failure is high at the boundary between the liquefied and non-liquefied ground for each cause of pipe failure. These findings agree with the experimental results presented by Kitaura and Miyajima (1983).

CONCLUSIONS

Response characteristics of pipelines located through both liquefied and non-liquefied ground were clarified based on mathematical analysis. The following can be concluded:

(1) One of the response characteristics of pipelines subjected to subsidence of ground is that the smaller the degree of liquefaction in the superficial ground, the greater the maximum bending pipe stresses. Moreover, the higher bending pipe stress occurs in areas of smaller width of the liquefied ground.

(2) The effects of buoyancy on pipe response are great in areas of great width of the liquefied ground and a high degree of liquefaction in the superficial ground.

(3) Resonance of the superficial layer of ground has great influence on the axial pipe strains during liquefaction processes. This suggests that great consideration should be given to vibration-induced strains during liquefaction.

ACKNOWLEDGMENTS

This study is supported in part by the Ogawa Foundation's Research Grant and the Grant-in-Aid for Scientific Research from Ministry of Education, Science and Culture of Japan.

REFERENCES

Kitaura, M. and Miyajima, M. 1983. Dynamic Behaviour of a Model Pipe Fixed at One End During Liquefaction, Proceedings of JSCE, No. 336, pp. 31-38 (in Japanese).

Kitaura, M. and Miyajima, M. 1985. Dynamic Behavior of Buried Model Pipe During Incomplete Liquefaction, Journal of Structural Engineering, JSCE, Vol. 31A, pp. 421-426 (in Japanese).

Kitaura, M. and Miyajima, M. 1986. Assessment of Safety of Pipelines Subjected to Soil Liquefaction, Preliminary Report of IABSE Symposium TOKYO 1986, Vol. 51, pp. 133-140.

Kitaura, M., Miyajima, M. and Suzuki H. 1987. Response Analysis of Buried Pipelines Considering Rise of Ground Water Table in Liquefaction Processes, Proceedings of JSCE, No. 380/I-7, pp. 173-180.

Lee, K. L. and Albaisa, A. 1974. Earthquake Induced Settlements in Saturated Sands, Proceedings of ASCE, Vol. 100, No. GT4, pp. 387-406.

Nishio, N., Tsukamoto, K. and Hamura, A. 1987. Model Experiment on the Seismic Behavior of Buried Pipeline in Partially Liquefied Ground, Proceedings of JSCE, No. 380, pp. 449-458 (in Japanese).

Yoshida T.and Uematsu, M. 1978. Dynamic Behavior of a Pile in Liquefaction Sand, Proceedings. of the 5th Japan Earthquake Engineering Symposium-1978, pp. 657-663 (in Japanese).

Yoshimi, Y., Kuwabara, F. and Tokimatsu, K. 1975. One-dimensional Volume Change Characteristics of Sands under Very Low Confining Stresses, Soils and Foundations, JSSMFE, Vol. 15, No. 3, pp. 51-60.

Table 1. Physical properties of steel pipe.

Outer diameter	(mm)	406.4
Thickness	(mm)	6.0
Young's modulus	(kgf/cm²)	2.1×10^6
Specific gravity		7.85

(1kgf/cm²=98kPa)

Table 2. Conditions of ground and magnitude of earthquake.

Longitudinal wave velocity c	170(m/s)
Period of shaking T	0.5(s)
Acceleration in superficial layer α	200(gal)
Displacement amplitude of non-liquefied superficial layer	$U_{s_0}=(T/2\pi)^2\alpha$

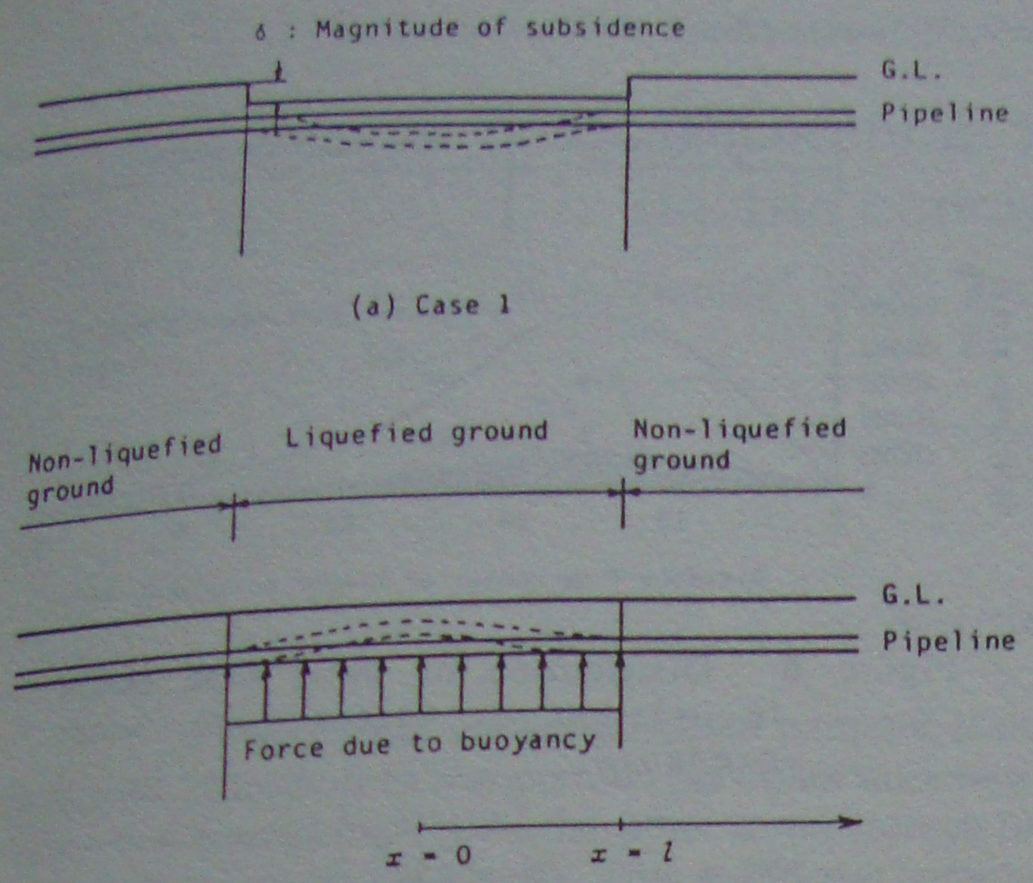

Figure 1. Analytical models for buried pipelines located between liquefied and non-liquefied ground.

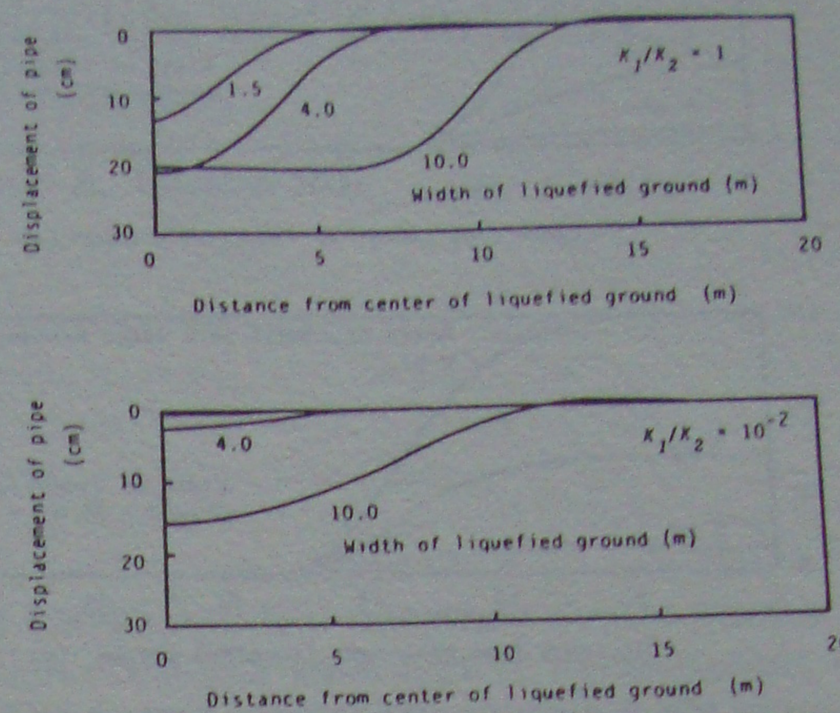

Figure 3. Distribution of pipe displacement due to subsidence.

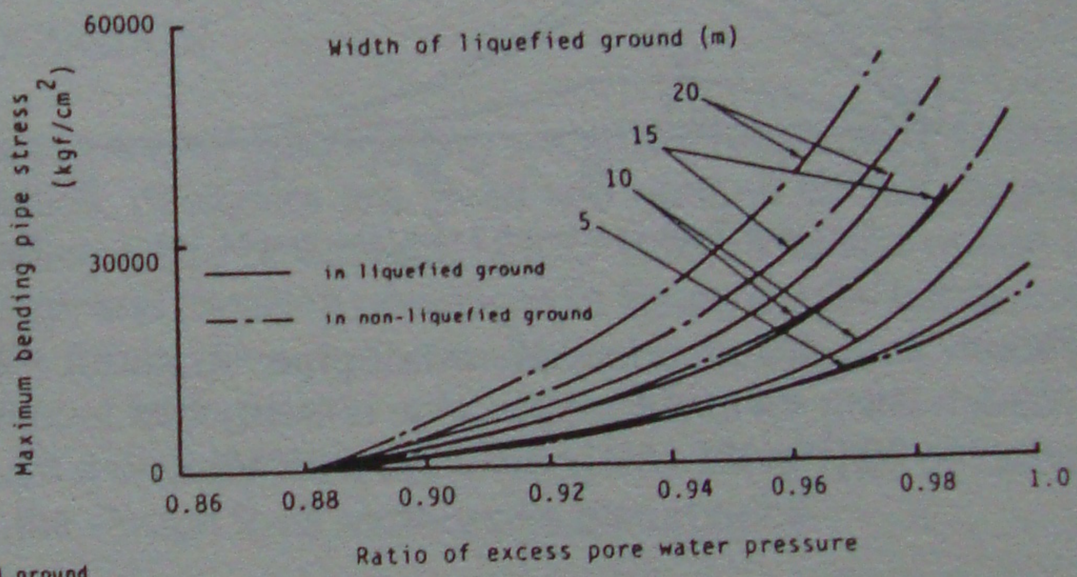

Figure 4. Relationship between maximum bending pipe stress due to buoyancy effects induced by liquefaction and excess pore water pressure ratio.

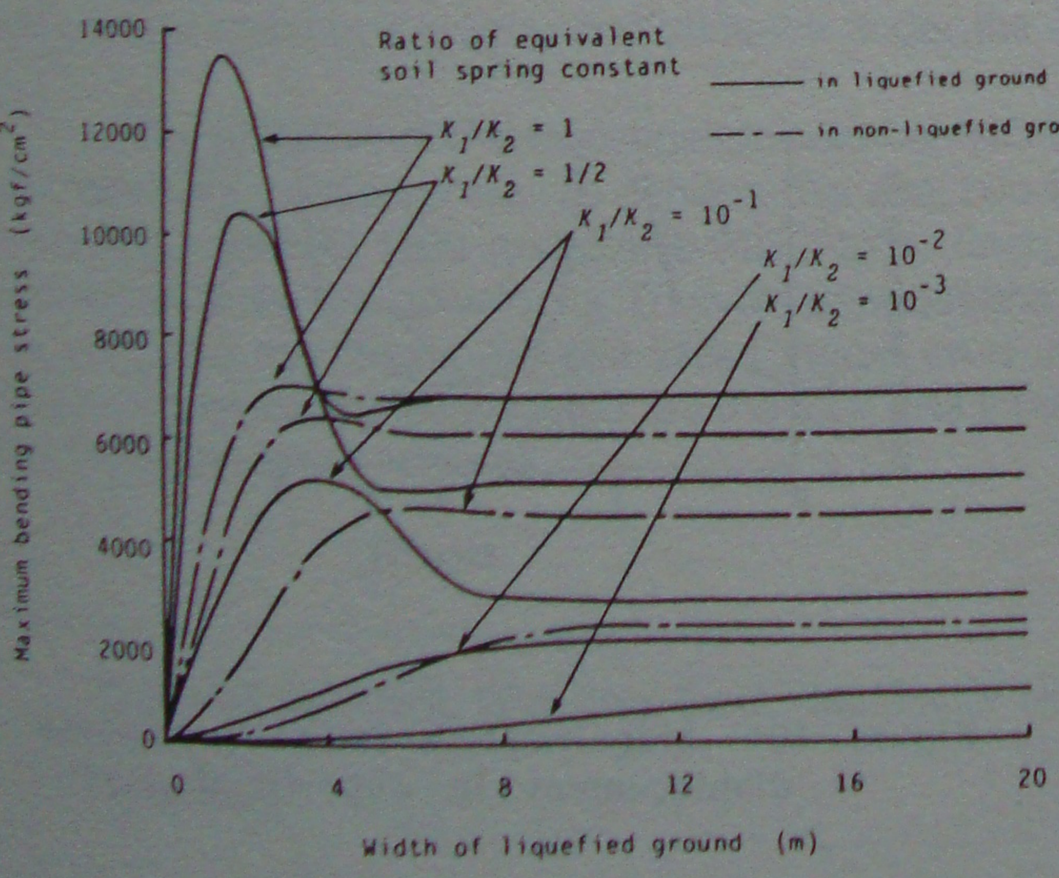

Figure 2. Relationship between maximum bending pipe stress due to subsidence of liquefied ground and width of liquefied zone.

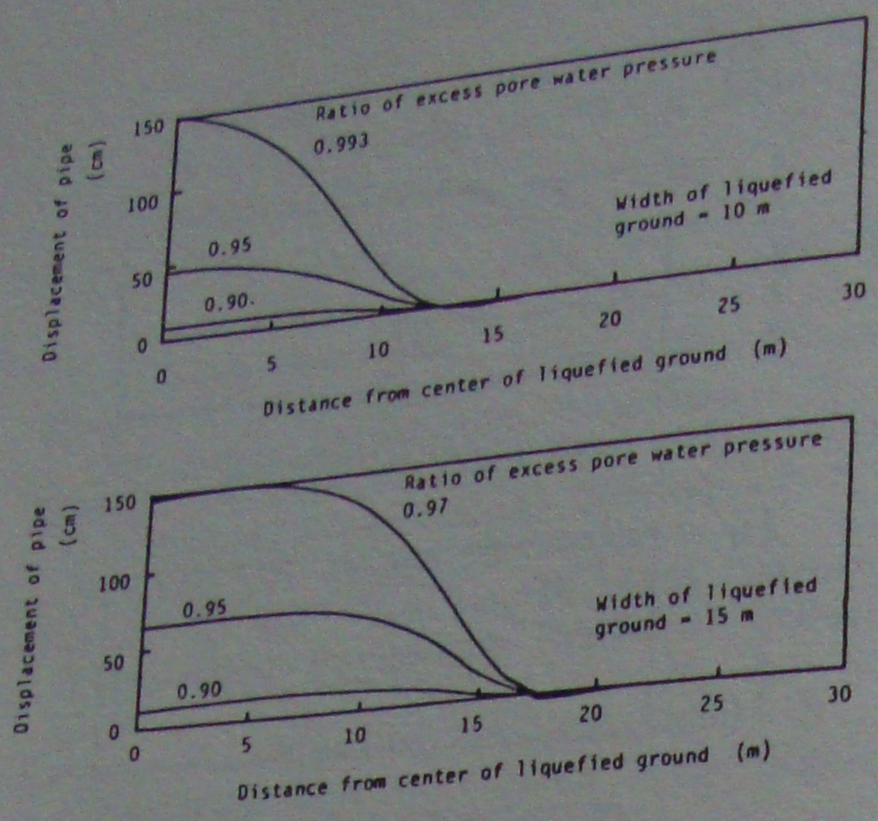

Figure 5. Distribution of pipe displacement due to buoyancy effects.

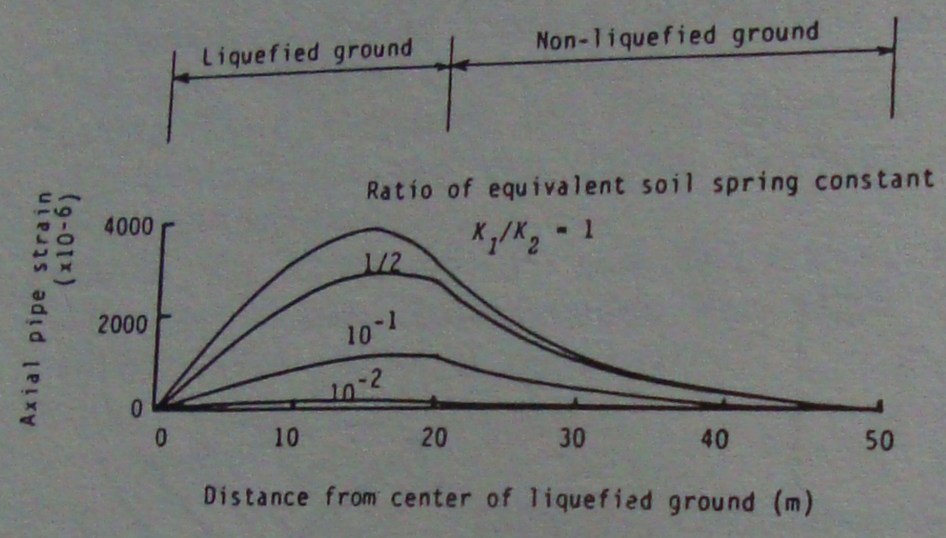

Figure 6. Distribution of axial pipe strain in relation to the ratio of equivalent soil spring constant.

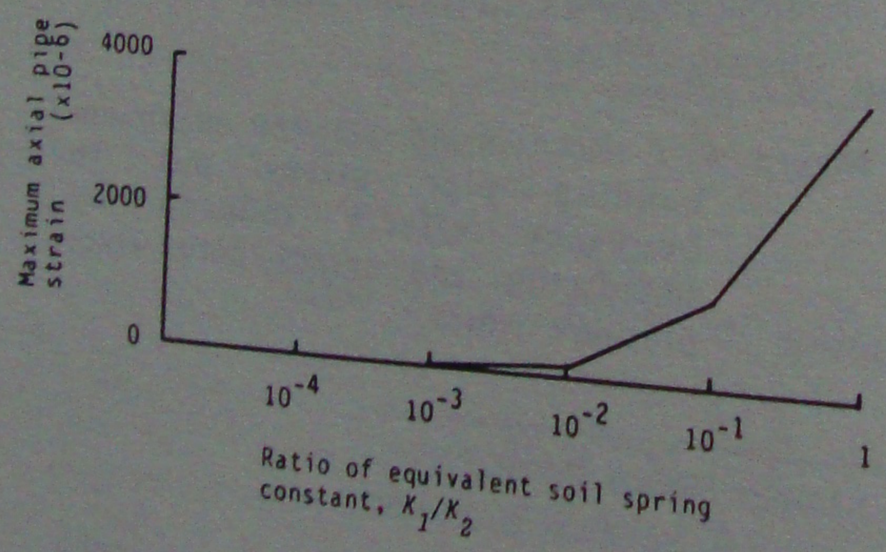

Figure 7. Relationship between maximum axial pipe strain and the ratio of equivalent soil spring constant.

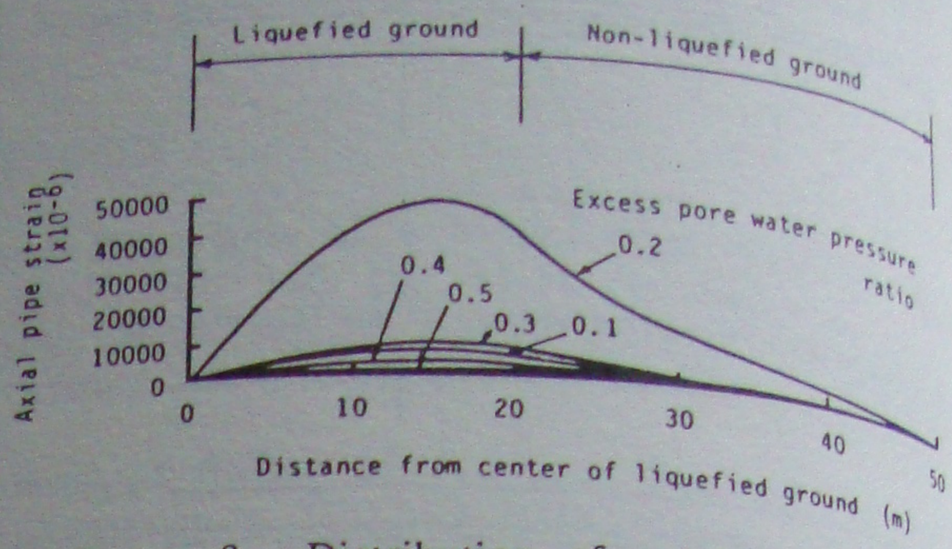

Figure 8 Distribution of axial pipe strain in relation to excess pore water pressure.

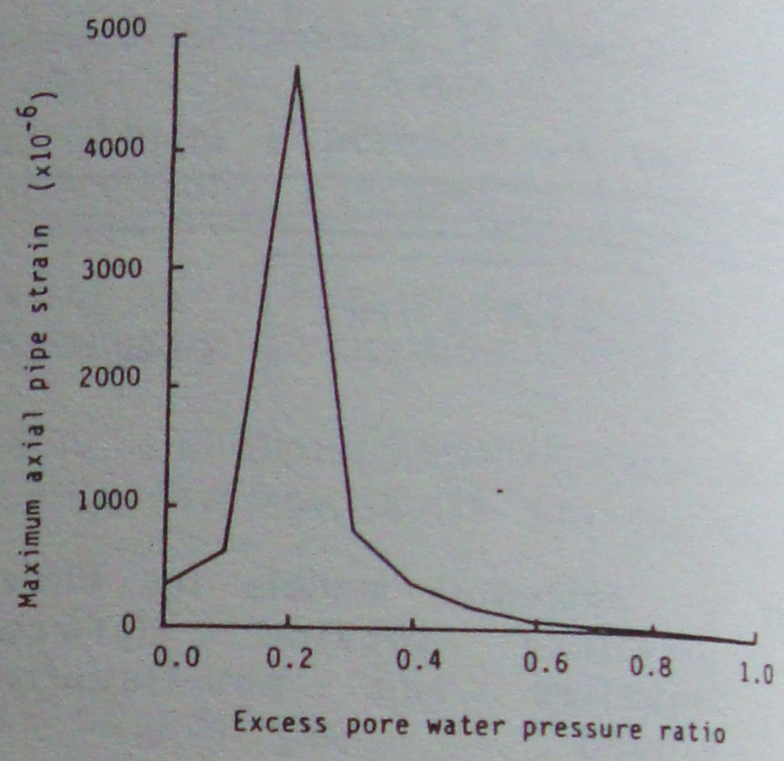

Figure 9. Relationship between maximum axial pipe strain and excess pore water pressure ratio.

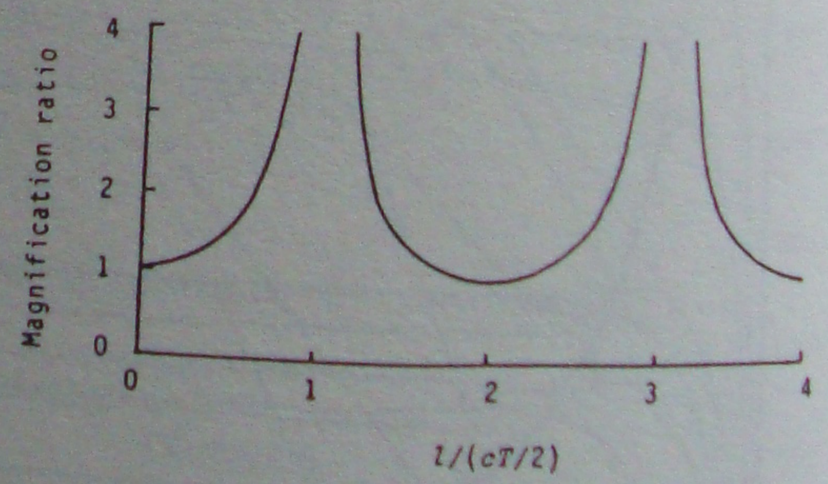

Figure 10 Magnification ratio of response displacement in superficial layer.